CEMB
Center for Engineering MechanoBiology

Penn
University of Pennsylvania

Summer 2022

Undergraduates Expanding Boundaries

Research Symposium

05 August 2022 | 09:00am ET

Glandt Forum, Singh Center

Meeting Link

Penn UExB
Research Symposium

05 August 2022 | 09:00am ET
Glandt Forum, Singh Center
Meeting Link

9:00-9:05	**Welcome, Annie Jeong, UExB Program Director**
9:05-9:18	**Rajal Vyas (West Chester University), Goldman Lab** Understanding the enzymatic activity of RNA helicases DDX3X and DDX3Y using multi-parameter confocal fluorescence spectroscopy
9:20-9:33	**Seth Ack (University of Puget Sound), Mauck Lab** Characterizing Meniscus Cell Mechano-Activation During Microgel Assisted Tissue Bulking
9:35-9:48	**Ellie Tanner (Purdue University), Boerckel Lab** Investigating the Spatial Expression of Putative YAP Target Genes in the Early Stages of Fracture Repair
9:50-10:03	**Milan Patel (New Jersey Institute of Technology), Boerckel Lab** Exploring Crosstalk between RhoA Signaling and YAP in Multiple Cell Types
10:05-10:18	**Rachel Achong (University of New Hampshire - Durham), Heo Lab** Impact of dECM:MeHA Hydrogel Stiffness on Bovine Meniscus Cell Phenotype
10:20-10:33	**Joseph Porter (East Tennessee State University), Lakadamyali Lab** Investigating the Preparation Methods for Super-Resolution Imaging of Tunneling Nanotubes
10:35-10:48	**Alex Coore (The University of Alabama), Janmey Lab** Mimicking Bioimpedance of Vocal Folds Through Phantom Models
10:50-11:03	**Garrett Hill (University of Maryland, Baltimore County,), Jain Lab** Investigating the Role of RNA Binding Proteins in Gene Expression
11:05-11:18	**Lauren Brown (University of Massachusetts Amherst), Svitkina Lab** Investigating Actin and Microtubule Crosstalk through Physical Linkage
11:20-11:33	**Lucas Sant'Anna (Northwestern University), Shenoy Lab** Integrating Cohesin Loop Extrusion-Mediated Transcription into a Chromosome Model
11:35-11:48	**Kelly Garcia-Ramos, University of Pennsylvania, Prosser Lab** Understanding LINC complex perturbations on cardiomyocyte force transmission and gene expression
11:50- 12:03	**Jakub Kowchanowski (Syracuse University), Ostap Lab** Exploring Drosophila Myosin-ID's Possible Interaction with DE-Cadherin
12:05	**Celebration luncheon** *open to all mentors, lab members, and attendees*

Understanding the enzymatic activity of RNA helicases DDX3X and DDX3Y using multi-parameter confocal fluorescence spectroscopy

By Rajal Vyas (Goldman Lab)

DDX3X and DDX3Y are sex-chromosome encoded RNA helicases that unwind double-stranded RNA for translation initiation. Even though the protein sequences of DDX3X and DDX3Y are 92 % identical, it has been previously found that these proteins have different RNA targets and different propensities to phase separate. Despite the fact that DDX3X has been previously studied, DDX3Y has not been studied in great depth, and this investigation will lay the foundation to further examine the enzymatic activities of these proteins in order to scrutinize the differences in catalytic activities that lead to their varying activities. We used multi-parameter confocal fluorescence spectroscopy (PicoQuant) and employed single molecule fluorescence resonance energy transfer (smFRET) assays to understand DDX3X and DDX3Y's RNA binding affinities and the dynamics of their ATP-dependent interactions with RNA. Using multi-parameter confocal technique we get access to various signals such as FRET and fluorescence fluctuations when the double-stranded RNA (dsRNA) labeled with Cy3 on the long strand and Alexa647 on short strand diffuses in and out of the detection volume. The obtained FRET signals were further analyzed using FRETBursts software to understand the enzymatic activity of DDX3X and DDX3Y, whereas the fluorescence fluctuations were auto-correlated to shed light on the distinct propensities of DDX3X and DDX3Y to phase separate by comparing the differences between the slowed diffusion rate of DDX3X and DDX3Y upon binding to RNA.

Characterizing Meniscus Cell Mechano-Activation During Microgel Assisted Tissue Bulking

Seth J. Ack,*[1,2,3] Ryan C. Locke,[1,4] Ryan N. Daniels,[1] Robert L. Mauck[1,2,3,4]
[1] Department of Orthopaedic Surgery, University of Pennsylvania, Philadelphia, PA
[2] Center for Engineering Mechanobiology, University of Pennsylvania, Philadelphia, PA
[3] Department of Biology, University of Puget Sound, Tacoma, WA
[4] Translational Musculoskeletal Research Center, Crescenz VA Medical Center, Philadelphia, PA,

Introduction: Due to limited vascular presence, inner zone tears of the meniscus have poor intrinsic healing capacity. Further, additional tissue deterioration following a partial meniscectomy is common, and has no clinical treatment options. Preliminary data shows the use of novel mechano-instructive hydrogel microparticles for facilitating meniscus wound closure via tissue bulking, an FDA approved acelluar therapeutic strategy. This strategy uses biocompatible hydrogels that are injected into a lesion to facilitate new tissue growth. Previous data showed that meniscus cells had increased cell spread and nascent matrix deposition when seeded on composite gels of norbornene-modified hyaluronic acid (NorHA) hydrogel microparticles encapsulated in bulk collagen. In this project, we further characterized the mechano-responsive activation of meniscus cells to NorHA microgels in order to enhance the clinical translation of this potential meniscus injury repair strategy.

Materials and Methods: 2D meniscus cell mechano-sensitivity confirmation: primary bovine meniscus cells (bMFCs) were cultured on polyacrylamide (PA) hydrogels with stiffnesses of 5 kPa, 55 kPa, and a glass positive control. Following 1d, cells were stained for Yes-associated protein (YAP) mechano-active transcriptional activator, actin (phalloidin-564), and nuclei (hoechst 33342) via immunofluorescence and imaged using confocal microscopy. Images were quantified for YAP nuclear localization, and cell shape, number, and density using Dragonfly software. Composite gel formulation: Soft (~5 kPa), stiff (~8 kPa), or no NorHA microgels (3wt%, NorHA, 2wt% fluorescein isothiocyanate green fluorophore, 0.05% LAP, 1mM RGDS, and variable DTT concentrations to control gel stiffness; fabricated using batch emulsion[2]) and bMFCs were encapsulated within collagen hydrogel (~2 kPa). Confocal: following 1d of culture, composite gels were stained, imaged, and analyzed as described above for PA gel experiments. Western blotting: following 1, 3, and 7d of culture, proteins were extracted from composite gels with RIPA buffer and separated on SDS-PAGE gels. Blots were transferred to PVDF membranes, treated with primary antibodies (YAP, anti-rabbit, ColI, anti-rabbit, Histone 3, anti-mouse), incubated in species-specific HRP-conjugated secondary antibodies, imaged using a ChemiDoc XRS Imaging System (BioRad), and analyzed using FIJI software. All statistical analysis was performed using PRISM software.

Results and Discussion: YAP nuclear localization is an indicator of cellular mechanoactivity.[2] There was a clear localization of YAP to the nucleus on the glass and 55 kPa substrates, as well as increased cell spreading on these substrates, compared to the soft substrate condition (Fig 1). Composite gels with stiff NorHA microgels had increased total cell number and cell spreading compared to gels with soft or no microgels (Fig 1). YAP nuclear localization increased when in proximity to both soft and stiff microgels, indicating meniscus cell mechano-activation in composite gels containing microgels (Fig 1). Global YAP protein expression did not significantly differ between conditions, which is potentially explained by heterogeneity in YAP subcellular localization in each composite gel. COL1 extracellular matrix (ECM) protein expression trended higher in composite gels with stiff microgels at 1d and 3d time points, indicating potential ECM repair capabilities of stiff NorHA microgels (data not shown).

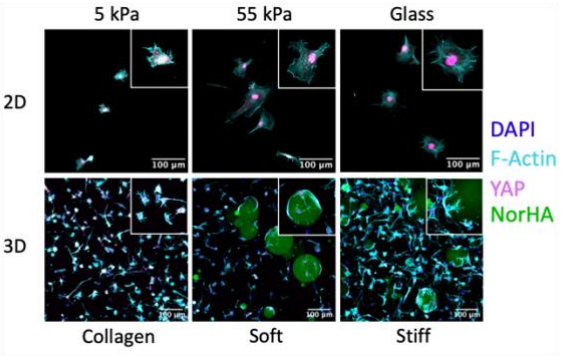

Figure 1. Meniscus cell mechano-activation on stiffer substrates. (Top row) bMFCs seeded on 2D substrates of varying stiffnesses. (Bottom row) bMFCs encapsulated in bulk collagen with no, soft, or stiff NorHA microgels.

Conclusions: Mechano-instructive hydrogels have the potential to activate meniscus cells, facilitating meniscus wound repair through increased cell proliferation, cell spread, and ECM protein production. This therapeutic strategy has high clinical translatability due to its simplicity of design and represents a potential treatment for dense connective tissue injuries.

Acknowledgments: This work was supported by the NIH/NIAMS (R01 AR071340, T32 AR053461, P30 AR069619) and the Department of Veterans' Affairs (I01 RX003375).

References:[1] Muir et al., ACS Biomater. Sci. Eng. 2021, 7, 4269−4281.[2] Dupont et al., Nature. 2011, 474, 179-183

Investigating the Spatial Expression of Putative YAP Target Genes in the Early Stages of Fracture Repair

Authors: Gabrielle I Tanner,[1,2,3] Madhura P Nijsure,[1,2] Annemarie Lang,[1] and Joel D Boerckel[1,2]
[1] Department of Orthopedic Surgery, University of Pennsylvania, Philadelphia, PA, USA, [2] Department of Bioengineering, University of Pennsylvania, Philadelphia, PA, USA, [3] Department of Agricultural and Biological Engineering, Purdue University, West Lafayette, IN, USA

Introduction: During bone fracture repair, some of the first responders are progenitor cells in the periosteum, the outermost layer of the bone. Though these periosteal cells are generally quiescent, they proliferate in response to a fracture because of a transcriptional co-regulator called Yes-associated protein (YAP). When a fracture occurs, YAP translocates to the nucleus of periosteal cells, becoming active and binding to other transcription factors to allow for gene expression and subsequent cell proliferation. When YAP is deleted from periosteal cells, they fail to sufficiently proliferate in the early stages of fracture healing, resulting in impaired bone regeneration (Kegelman, 2020). However, the specific proteins YAP transcribes in the context of periosteal cell proliferation remain unknown. We therefore used bulk mRNA sequencing to identify putative YAP target genes involved in this proliferation and spatially mapped the protein level expression of two of these genes in the early fracture callus by immunofluorescence staining.

Materials and Methods: We evaluated protein level expression of BMP4 and IL11 in the fracture callus of 14- to 16-week-old Osterix-conditional YAP/TAZ knockout (KO) mice (n=3) and their wild type (WT) littermates (n=3). We also stained for Osterix and YAP to map the regions where the Osterix-conditional YAP/TAZ knockout took effect. We activated the adult-onset KO in the mice two weeks prior to fracture surgery, then induced femoral fractures using an intramedullary pin for stabilization. We harvested and fixed the intact and fractured limbs four days post-fracture, then decalcified them for two days. We then cryo-embedded the samples in Tissue-Tek OCT resin and cryosectioned them using tape according to previously established protocols (Dyment, 2016). We blocked and permeabilized the sections using 1X PBS with 5% goat serum and 0.3% Triton X-100, then stained them with antibodies corresponding to the proteins of interest. Finally, we used immunofluorescence imaging to determine the location and intensity of the proteins throughout the sample, specifically in the periosteum.

Results and Discussion: Image processing for this project is still ongoing, but we hypothesize that it will reveal reduced protein expression levels of BMP4 and IL11 in the periosteum in KO mice compared to their WT littermates. We also acknowledge that this effect may not be observable in the current sample size. In light of this, data collection is also ongoing.

Conclusions: Our initial troubleshooting resulted in a reproducible protocol for evaluating the protein level expression of putative YAP target genes in the early stages of fracture repair in WT and KO mice. In the event that our hypothesis is correct, we will proceed to testing whether they can rescue the effect of YAP in a KO model. Alternatively, we are continuing to investigate the protein expression of other putative YAP target genes identified by the aforementioned bulk RNAseq.

Acknowledgements: This work was supported by the Center for Engineering MechanoBiology (CEMB), an NSF Science and Technology Center, under grant agreement CMMI: 15-48571, as well as the McKay Orthopedic Research Laboratory, University of Pennsylvania, under NIH grant agreement R01-AR073809.

References: Dyment, N.A. et al., *J.Vis.Exp.*, (2016), (115); Kegelman, C.D. et al., *JBMR*, (2020), *32*(1) 143-157.

Exploring Relationships between RhoA Signaling and YAP in Multiple Cell Types

Authors: Milan Patel, Annapurna Pranatharthi Haran, Joel D. Boerckel
Affiliations: Center for Engineering MechanoBiology, University of Pennsylvania; Department of Bioengineering, University of Pennsylvania; Deptartment of Orthopaedic Surgery, University of Pennsylvania

Introduction:

To be able to repair tissues, one must understand the intracellular proteins and pathways that direct cell growth and movement. Transcriptional coregulator Yes-associated protein (YAP) is one protein that upregulates cell proliferation. RhoA, a GTPase involved in reorienting the cytoskeleton to facilitate cell movement, is known to regulate YAP, but little is known about how it does this. To better understand the interactions between these proteins, we utilized optogenetics, which involves modifications of proteins to become light sensitive. To this effect, genes for an Opto-RhoA tool have been created and experimented with. We used this tool to observe what occurs when RhoA signaling is activated, and to better understand the relationship between RhoA, YAP, and cell proliferation and movement.

Materials and Methods:

Opto-RhoA is created by combining RhoA with a photoreceptor protein (BcLOV4) and a staining protein (mCherry), so that the tool can be light activated and seen with fluorescence microscopy. Using DNA isolated from bacterial plasmids for Opto-RhoA, human embryonic kidney cells (HEKs) and UMR-106 cells were transfected with Opto-RhoA and first observed live using fluorescence microscopy. Cells were quickly exposed to EGFP light and observed to note changes in morphology and Opto-RhoA localization. After live imaging, cells were fixed and immunostained to locate YAP, nuclei, and actin in the cells. Using images of these fixed cells, we compared cells with and without induced RhoA activation to see if YAP localized in different locations.

Results and Discussion:

From live imaging, we found that activation of RhoA causes membrane localization of RhoA, as well as breaking of cell-cell and cell-ECM adhesions, which facilitated contraction in these cells. Light activated cells without Opto-RhoA demonstrated no movement. From the fixed-cell images, we noted that RhoA activated cells had higher concentrations of nuclear YAP and lower concentrations of cytoplasmic YAP (see Figure 1). Higher nuclear YAP leads to the transcription of proliferative proteins, and therefore higher probability of cell proliferation. These findings show that activation of RhoA signaling induces cell contraction and proliferation.

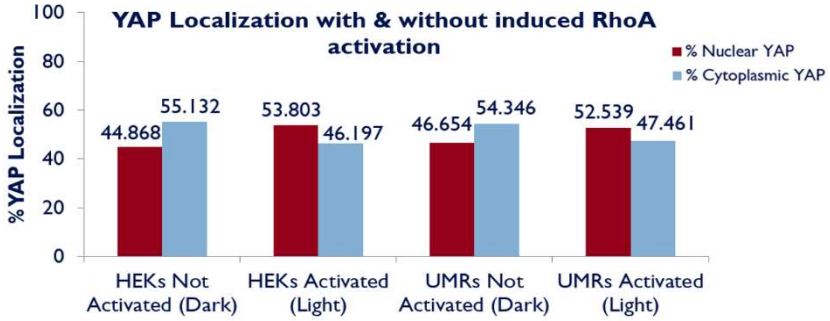

Figure 1. Graph of YAP localization by area (Nuclear YAP in maroon, Cytoplasmic YAP in blue) in HEK cells (left) and UMR cells (right) with and without RhoA activation. RhoA activated cells were found to have higher nuclear YAP and lower cytoplasmic YAP.

Conclusion:

These experiments demonstrated that RhoA activation seems to facilitate YAP acting as a transcriptional coregulator by helping localize YAP to the nucleus. We also observed that RhoA activation promotes cell contraction and may help regulate proliferation. These findings help solidify a relationship between RhoA and YAP and confirm these proteins as key factors in the proliferative and movement processes of the cell. The applications for these proteins in wound healing and bone fracture repair increase notably with these findings.

Acknowledgements:

This work was supported by the Center for Engineering MechanoBiology (CEMB), an NSF Science and Technology Center, under grant agreement CMMI: 15-48571.

Impact of dECM:MeHA Hydrogel Stiffness on Bovine Meniscus Cell Phenotype

Rachel Achong [1, 2, 3, 4], Se-Hwan Lee [1, 2],Yujia Zhang [1, 2, 3], Zizhao Li [1, 2,], Su-Chin Heo [1, 2, 3]

1. Department of Bioengineering, School of Engineering and Applied Science, University of Pennsylvania, Philadelphia, PA

2. McKay Orthopaedic Research Laboratory, Department of Orthopaedic Surgery, Perelman School of Medicine, University of Pennsylvania, Philadelphia, PA

3. Center for Engineering Mechanobiology, University of Pennsylvania, Philadelphia, PA

4. Department of Molecular, Cellular, and Biomedical Sciences, College of Life Sciences and Agriculture, University of New Hampshire, Durham, NH

Human meniscus tears affect over 1 million individuals in the United States each year, but the avascularity of the meniscus limits its capacity to self-heal from injury. Therefore, an effective solution is required to restore the function and health of menisci. Biomaterials are a promising alternative to meniscectomies, by repairing the injured site, recruiting native cells for growth and repair, and salvaging the healthy meniscus instead of replacing it entirely. To gain insight on potential biomaterial treatments, we investigated the phenotypic effect of hydrogel stiffness on meniscus cell phenotype. To achieve this, a tunable hydrogel system was developed to promote meniscus cell adhesion, morphology, and proliferation, while controlling for the stiffness of the hydrogels to observe its phenotypic impact on juvenile bovine meniscus fibrochondrocytes (jBMFCs). This was achieved by using bovine decellularized extracellular matrix (dECM) as the medium for promoting cellular activity, and using methacrylate functionalized hyaluronic acid (MeHA) to adjust the stiffness of the hydrogels through polymeric crosslinking. dECM is a promising biomaterial for tissue repair because it contains essential proteins, such as collagen and RGD, which facilitate normal cell activity. Hyaluronic acid is a crucial component of the extracellular matrix, particularly for its role in wound healing; it was functionalized with methacrylate to provide a capacity for chemical crosslinking. The phenotype of the jBMFCs was characterized by the cells' adhesion, morphology, and proliferation within the dECM:MeHA hydrogels. To synthesize the dECM:MeHA hydrogels, 1.5% dECM solution was combined with various concentrations of MeHA (0.5-1.0%). The combined solution was crosslinked under ultraviolet light and heat (37°C). Following hydrogel synthesis, well-plate samples were seeded with jBMFCs for *in vitro* testing. After growth, they were compared to native meniscus tissue for cell adhesion and morphology in the dECM:MeHA hydrogel through actin staining and visualization, and their rate of proliferation was analyzed through Cell Counting Kit 8 assay (CCK-8). Unseeded dECM:MeHA hydrogel samples were analyzed for their mechanical properties, specifically compression, for future comparison to the biomechanics of native bovine meniscus tissue. The jBMFCs exhibited striated morphology along with greater adhesion and growth within the stiffer 1.5% dECM: 1.0% MeHA hydrogels compared to the softer 1.5% dECM: 0.5% MeHA hydrogels. This indicates the stiffer hydrogel promoted more favorable cell activity by mimicking the extracellular environment and mechanical properties of native bovine meniscus tissue through a higher concentration of crosslinked MeHA. This provides insight into regenerative biomaterial treatments for meniscus injuries, and preliminary data on the importance of biomaterial stiffness on cell activity and success.

Investigating the Preparation Methods for Super-Resolution Imaging of Tunneling Nanotubes

Joseph Porter, Qing Tang, Melike Lakadamyali

Tunneling nanotubes are long-range, membrane enclosed tubular structures spanning from cell-to-cell that can mediate intercellular communications and transfer of organelles, viruses, and protein aggregates across many microns. The major cytoskeleton component responsible for this transfer are linear actin bundles that span the entire length of the nanotube, connecting the cytoplasm of each cell. Despite the near two decades of study into nanotubes, the understanding of their formation and organization is limited. Tunneling nanotubes regularly measure under 700 nm in diameter but can measure up to 200 μm in length; the thin, fragile nature of these structures cause them to easily become disrupted during fixation processes and inhibit their study. The goal of this study was to establish methods that allow us to observe organizations of actin within tunneling nanotubes at nanoscale using super-resolution microscopy. The study tested a range of cell confluency, fixation and permeabilization conditions for establishing and preserving nanotubes between U2OS cells and used Alexa-647 phalloidin to label actin filaments for stochastic optical reconstruction microscopy (STORM) imaging. We found that gentle, multi-step fixation and low-degree permeabilization gave the best results at preserving long and thin cellular protrusions, such as filopodia, which are considered potential precursors of nanotubes, as well as nanotube-like structures connecting between cells.

Mimicking Bioimpedance of Vocal Folds Through Phantom Models

Author: Alexis Coore (The University of Alabama Department of Mechanical Engineering)

Introduction: In the United States, over 6 million citizens have been diagnosed with some form of neurodegenerative disorder (NDD), which is any illness that targets the central nervous system. Around a third of this population can be categorized as traumatic neurodegenerative disorders, which includes ailments such as some cancers, strokes, and spinal cord injuries. This subset of NDDs are more likely to cause excessive physical damage to the brain. Full recovery from this is highly unlikely, due to the development of scar tissue at the base of the injury. Hydrogels are proving to be ideal in reducing the amount of scarring produced, but must be tailored to specific biophysical needs. Our research focuses on cultivating the optimal hydrogel for this purpose.

Materials and Methods: The primary components of our hydrogels include Chitosan and Polyaniline (PANI). Chitosan is a chemical compound found in shellfish and was chosen for its ideal physical properties. It is non-immunogenic, antibacterial, and biodegradable, meaning it will dissolve in the patient's body without the need for additional surgery. PANI is a conductive polymer, which gives us greater control over drug delivery. These two elements are grafted together and allowed to dry fully. Our lab tests each hydrogel for stiffness, roughness, conductivity, and bacteriology. An Atomic Force Spectrometer is used for both stiffness and surface roughness. Because the final form of these hydrogels has not been decided, we aim to make our gels pliable and relatively smooth, in the hopes that multiple avenues of application are possible. A handheld multimeter is used for conductivity measurements. This aids us in deciding which concentration of PANI will work best once the final stages of testing are reached. Finally, we test for how the hydrogels interact with bacteria. We cultured both Pseudomonas aeruginosa and Staphylococcus aureus for placement on the hydrogels, as these are two of the more common strains found in human patients. Because the gels have a heightened conductivity, we also ran assorted voltages through the hydrogels.

Results and Future Directions: As the project is still in its early stages, our research revolved around running various trials and mapping out the results. We have found that, although we are sure of the components of the hydrogel, it is unclear how long they should be allowed to dry for. If the time is too short, we risk disintegration, but if it is left for too long, the gels may become too thin to test. In addition to this, we have found that though conductivity across concentrations is stable, the level we are striving for is unknown. In the future, we hope to find the optimal amounts for each. Our most conclusive result laid in the bacteriology tests. No matter what voltage we used, including the lack thereof, no bacteria attached itself to the hydrogels. It is also of note that even the slightest amount of electricity impeded the development of bacteria colonies. This conveys that our hydrogels will not attract any bacteria to the wound, and reduces concerns of infection.

Investigating the Role of RNA Binding Proteins in Gene Expression

Garrett Hill[1], Zachary Gardner[1], Rajan Jain[1]
[1]Department of Medicine, Perelman School of Medicine, University of Pennsylvania.

Introduction: Friedreich's ataxia (FDRA) is an autosomal recessive disorder affecting 1 in 50,000 people that causes progressive nervous system damage and impaired movement. Molecularly, this disorder is characterized by abnormalities in the frataxin gene (*FXN*), which encodes for an iron chaperone protein important for iron-sulfur cluster biogenesis in the mitochondria. In unaffected people, the first intron of *FXN* contains 7-35 repeats of the nucleotide sequence GAA. In people with FRDA the first intron of *FXN* contains several hundred GAA repeats (Cook & Giunti, 2017). This repeat expansion results in a decreased *FXN* expression and localization of the locus to the nuclear periphery. It is important to note that generally, genes located at the nuclear periphery are contained in heterochromatin and have decreased expression.

Interestingly, it has been previously demonstrated that Serine and arginine-rich (SR) proteins, RNA binding proteins which play a critical role in the assembly of the spliceosome during mRNA processing, have a GAA-rich binding sequence. To assess the relationship between SR protein binding and expression of *FXN* in FRDA cell lines, we propose a model in which excess GAA repeats in the *FXN* transcript act as a sink for SR proteins. Excess SR protein binding decreases the stability of the mRNA and lowers *FXN* expression. This project aims to validate this mechanism and investigate more generally the relationship between SR proteins, gene expression, and chromatin organization.

Materials and Methods: To verify this model, we knocked down SR protein expression in FRDA and wild-type cell lines and then examined the expression of *SRSF1* (a gene encoding for a candidate SR protein) and *FXN*. Knockdown of SRSF1 was achieved through exogenous expression of shRNA, which binds to *SRSF1* mRNA and targets it for degradation. We utilized viral infection of target cells to enable the expression of shRNA. Once infected, lentivirus integrated targeted shRNA with the cell genome, triggering shRNA expression. After infection was achieved, *FXN* and *SRSF1* mRNA expression levels were analyzed using qPCR to verify knockdown efficiency and examine *FXN* expression dynamics.

Results and Discussion: After qPCR analysis of wild-type and FRDA cell lines with and without SRSF1 knockdown, it was found that there was no significant change in *FXN* expression in the wild-type strain or the FRDA model cell line with the SRSF1 knockdown, as seen in figure 1. This suggests that the binding of SRSF1 to repeat expanded *FXN* mRNA transcripts has no effect on *FXN* transcription levels or that excess SRSF1 binding does not occur.

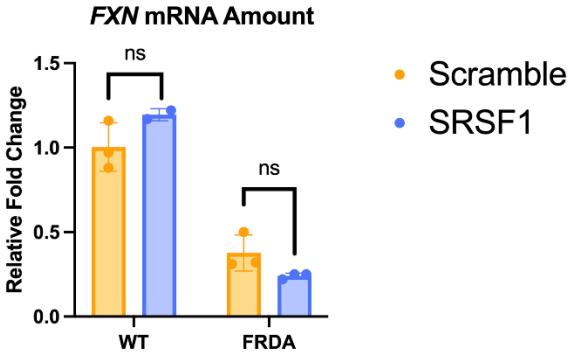

Figure 1. Quantification of FXN mRNA levels in the wild type (WT) and Friedrich's ataxia (FRDA) cell lines infected with a scramble control virus and an SRSF1 knockdown virus.

Conclusion: While current mechanisms for the repression of *FXN* expression in those with Friedrich's ataxia have already been described, this project aimed to elucidate a potentially novel mechanism for transcriptional repression. Ultimately, however, our data is consistent with the conclusion that SR proteins play little to no role in regulating *FXN* expression and this model for repression is most likely not relevant in FRDA cell lines. To further develop this relationship, future experiments will utilize cross-linking immunoprecipitation (CLIP) assays to determine if SRSF1 binding is occurring at the *FXN* transcript. This will help determine if excess SRSF1 binding is not having any effect on transcription or if this excess binding is not occurring in the first place.

References

(1) Cook A, Giunti P. Br Med Bull. 2017;124(1):19-30

Investigating Actin and Microtubule Crosstalk through Physical Linkage

Authors: Lauren Brown[1], Xingyuan Fang[2], Tatyana M. Svitkina[2]
[1]Center for Engineering Mechanobiology, University of Pennsylvania [2]Department of Biology, University of Pennsylvania

Introduction: Cell motility and directional migration are necessary for cellular functions, while abnormal motility leads to diseases, such as cancer metastasis. Individual cell polarity creating distinct front and back ends needs to be established for cell movement and can be regulated through cytoskeleton components. The cytoskeleton, made of actin, microtubules and intermediate filaments is critical for cell structure and motility. Actin filaments are enriched at the cell leading edge in the form of branched networks in lamellipodia, where they generate force for cell protrusion. Microtubules are distributed throughout the cell and are thought to have a more global role in cell motility by "managing" actin roles in time and space. A leading question of our research is to investigate how microtubules control cell motility. Current models suggest that microtubules deliver "protrusion factors" to the leading edge, are involved in Rho GTPase regulation, and promote disassembly of focal adhesions, yet fail to show a direct link between microtubules and cell protrusion. Electron microscopy images have shown association of branched actin filaments with microtubules in neurons, suggesting that microtubules initiate assembly of these branching networks[3]. This research aims to provide evidence for microtubule associated branched actin at the cell leading edge of non-neuronal cells, and thus for a direct mechanism of microtubule controlled cell protrusion through branched actin formation at the microtubule tip.

Materials and Methods: COS-7 cells were cultured in DMEM containing 10% FBS. Latrunculin B (LatB) in DMSO, an actin depolymerizing agent, was used to clear excess actin and allow for visualization of microtubule tips at the dense branched actin areas. Cells were treated with DMSO as a control, 2.5µM LatB, or 5µM LatB for one hour. Samples for confocal microscopy were fixed and stained with fluorescent phalloidin to detect actin filaments and α-tubulin antibody to reveal microtubules. Samples for platinum replica electron microscopy (PREM) were processed according to protocol and imaged using transmission electron microscopy[4].

Results and Discussion: DMSO treated control cells in Fig.1A were well-spread and contained microtubules and actin filaments distributed throughout the cell. Cells treated with 2.5µM or 5µM LatB contracted after treatment and exhibited processes extending outward from cell bodies. Fig.1B shows actin (orange) at microtubule tips (green) after 2.5µM LatB treatment for 1 hour. Increasing the concentration of LatB to 5µM for 1 hour produced greater contracted cells with longer processes. Fig.1C shows PREM imaging of a 2.5µM LatB treated cell showing branched actin filaments along microtubules. Branched actin networks were densely concentrated making them difficult for visualization under PREM imaging. Fig1D shows branched actin network formation observed at a microtubule tip in a cell treated with 5µM.

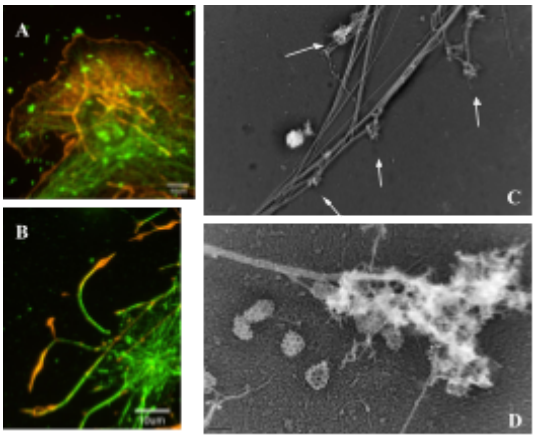

Figure 1. (A) Confocal image of DMSO treated COS-7 cell fixed with 0.2% GA (B) Confocal image of 2.5 µM Lat B treated cell fixed with 4% PFA showing branched actin (orange) at microtubule tips (green) (C) PREM image of 2.5 µM Lat B treated cell showing branched actin formation along microtubules (D) PREM image of a branched actin network formed at a microtubule tip in cell treated with 5µM Lat B.

Conclusions: In this study we demonstrate that a subpopulation of microtubules was associated with branched actin network at their tips at the cell periphery, which likely leads to microtubule-controlled leading edge protrusion. This work provides a new model for investigation of direct microtubule involvement in cell motility and migration. Further work may provide evidence of a linker physically joining actin and microtubules.

Acknowledgements: This project was supported by the NSF-funded STC, CEMB, award number CMMI-1548571.

References: [3] Nadia Efimova et al. Branched actin networks are assembled on microtubules by adenomatous polyposis coli for targeted membrane protrusion. *J Cell Biol* 7 September 2020 [4] Svitkina T. Imaging Cytoskeleton Components by Electron Microscopy. Methods Mol Biol. 2016

Integrating Cohesin Loop Extrusion-Mediated Transcription into a Chromosome Model

Lucas E. Sant'Anna[1,2], Vinayak Vinayak[2,3], Aayush Kant[2,3], and Vivek Shenoy[2,3]
[1] Department of Biomedical Engineering, Northwestern University. [2] Center for Engineering MechanoBiology, University of Pennsylvania. [3] Department of Material Science and Engineering, University of Pennsylvania.

Introduction: Chromatin—the combination of protein and DNA that makes up the chromosome—exhibits a highly dynamic and complex structure that plays a central role in nearly all aspects of eukaryotic biology. Chromosomes have been shown to undergo dynamic reorganization in response to external stimuli, which can cause genome-wide changes in expression[1]. Epigenetic modifications like acetylation and methylation are thought to control these changes in packing, which influences which genes are suppressed and which are expressed by modulating their epigenetic state, such as heterochromatin or euchromatin, and in turn their accessibility to transcriptional machinery. However, active gene transcription has also been shown to affect the packing structure of DNA and reduce heterochromatic domain size[2]. Physical modeling of chromatin with molecular dynamics engines has shown significant promise in understanding chromatin structure[3], and we are interested in expanding these models to be able to predict how DNA structure changes in response to epigenetic and transcriptional dynamics. Here, we implement an implicit model for cohesin loop extrusion-mediated transcription into our model of the chromosome to recapitulate the effects of transcription on epigenetic dynamics and packing structure of chromatin.

Materials and Methods: In this work, we model the chromosome as a copolymer of two different epigenetic states, heterochromatin and euchromatin. These simulations are conducted in the Large Atomic/Molecular Massively Parallel Simulator (LAMMPS), an open-source molecular dynamics software package developed by Sandia National Laboratories[4]. Cohesin loop extrusion-mediated transcription was modeled implicitly by a probability described by equation 1, where P_{ext} is the probability of loop extrusion, h is the number of heterochromatin neighbors, Γ is the transcription rate, and h_{max} and Δh are parameters that can be optimized to fit experimental data.

$$P_{ext} = \Gamma\left(1 - \frac{\Delta h^{\left(\frac{h_{max}}{2} - h\right)}}{1+\Delta h^{\left(\frac{h_{max}}{2} - h\right)}}\right), \qquad (equation\ 1)$$

The model of the chromosome also incorporates the physics of chromatin-chromatin interactions, epigenetic diffusion, and epigenetic regulation, whose governing equations and models have been validated in previous work[1].

Results and Discussion: Culturing cells with Actinomycin D (ActD) results in transcriptional inhibition. Super resolution microscopy (STORM) images of transcriptionally inhibited cells demonstrate increased heterochromatic domain size compared to control cells. Qualitative comparison of STORM images with our model shows agreement where transcriptional inhibition reproduces this phenomenon (Figure 1a). Moreover, increasing transcription rate produces a relatively linear decrease in heterochromatic domain size (Figure 1b), which mirrors the behavior of our phase-field model of the chromosome (unpublished). We conclude that our model for cohesin loop extrusion could explain the link between increased transcription rate and decreased heterochromatic domain size observed in cells.

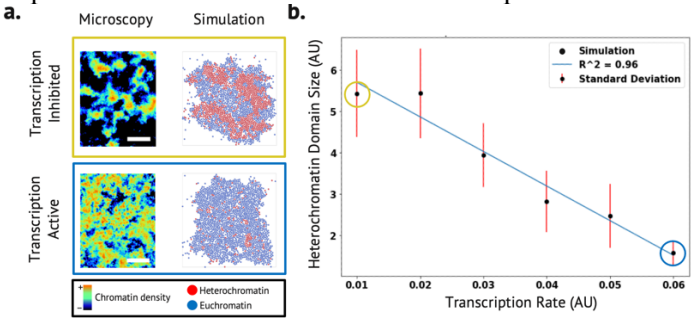

Figure 1. Our model for cohesion loop extrusion-mediated transcription recapitulates the observed phenomenon in cells in our model of the chromosome. (a) Cell images and model images from transcriptionally active and inhibited states. STORM imaging was used to produce cell images, where red represents the densest chromatin. Scale bar 1 μm. (b) Heterochromatic domain size from our simulation plotted against transcription rate, producing a linear trend.

Conclusion: Further utility from this model could arise from implementing our model for transcription into a full chromosome copolymer model, where initial epigenetic states are derived from ChIP-Seq data. Ultimately, these refinements would advance our model towards the ability to explain and predict epigenetics-controlled changes in gene expression, which could enhance our understanding of key biological processes such as embryonic development and metastasis of cancer.

Acknowledgements: This work was supported by the NSF-funded STC, CEMB (award number CMMI-1548571).

References: (1) Heo, S.J. *Nat. Biomed. Eng.*, 2022, 910. (2) Neguembor, M.V. *Mol. Cell*, (2021), 81(15), 3065-3081. (3) Shi G., *Nat. Commun.*, 2018, 9, 3161. (4) Thompson, A.P., *Comput. Phys. Commun.*, 2022, 271.

UNDERSTANDING LINC COMPLEX PERTURBATIONS ON CARDIOMYOCYTE FORCE TRANSMISSION AND GENE EXPRESSION

Authors: Kelly Garcia-Ramos, Daria Amiad-Pavlov, Lauren Testa, Benjamin Prosser
Perelman School of Medicine, Department of Physiology, University of Pennsylvania, 415 Curie Blvd, Philadelphia, PA 19104

Introduction: Cardiomyopathy is a cardiac muscle-related condition that is the most common cause of sudden-death in young people (30 years or less)[1] and has been associated with cardiomyocyte (CM) mutations in LINC complex proteins, which weaken the nuclear envelope. ***Studies have shown that mechanical forces on the heart throughout life have an effect on the cytoskeletal-nuclear interactions of CMs.*** Deformations in the nucleus causes genome reorganization, increasing patient propensity to cardiomyopathy. However, disrupting force transmission via the LINC complex is found to compensate for weakened nuclear membrane, increasing lifespan.[2] We have found that cells containing nesprin-1 protein in the nuclear membrane with a dominant negative KASH domain (DN-KASH) (affecting membrane/LINC complex) have decondensed peripheral chromatin relative to control cells.

Methods: We isolate our cardiomyocytes from rats and keep them in cell media. Then, we use a null and DN-KASH virus to infect our cell lines. Confocal imaging with immunofluorescence will allow us to see disruption of the KASH domain with infection of cells with DN-KASH virus after 48 hours. and differences in h3k9me2 marker concentration. Now we want to observe the specific protein to protein interactions that are responsible for this change in force transmission to chromatin via PLA or Proximity Ligation Assay by incubating our cells in Duolink probe, ligation, and amplification buffers.

Results and Discussion: In null cells, lamin B is more concentrated at the nuclear periphery and H3K9me2 markers aren't as strong as opposed to DN-KASH. From figure 1, cells with a perturbed DN-KASH membrane have less lamin B due to increase in surface area, and higher signal of methylation, especially around the periphery. Using Proximity Ligation Assay (PLA), in DN-KASH cells, there's a significantly higher number of punctae around the nuclear periphery, suggesting interactions in disrupted LINC cells.

Conclusions: There is quantifiable evidence that forces exerted on the nucleus by the cytoskeleton are important in maintaining chromatin compaction, and thus the accessibility of DNA to transcription factors due to hyperacetylation or hypomethylation around histones. Even though we anticipate to see changes between the size and applied force of the nucleus in null and DN-KASH live cells, there could be conflicting data with DN-KASH and DNA organization. Live DN-KASH cells show that DNA in nuclear periphery is less compact at the membrane, but with fluorescence in fixed cell cultures, the markers of compaction (H3K9me2) are more expressed, meaning more repressed genes.

---

[1] Cardiomyopathy. *Centers for Disease Control and Prevention* (2019).

[2] Chai, R. J. *et al.* Disrupting the LINC complex by AAV mediated gene transduction prevents progression of lamin induced cardiomyopathy. *Nature Communications* **12,** (2021).

Exploring *Drosophila* Myosin-ID's Possible Interaction with DE-Cadherin

Authors: Jakub A. Kochanowski*, Faviolla A. Baez-Cruz, E. Michael Ostap

Introduction: Chirality is the property of structures to hold shapes in which a rotation cannot produce its mirror image, seen in human hands or positioning of the heart. Chirality exists on all scales, from molecules all the way to the structure of full organisms. During development, chirality is essential for the proper positioning and twisting of organs, enabling their function. The understanding of its emergence and establishment is crucial to understand cellular mechanics, a field which has recently shown much growth in interest and discoveries. However, the underlying mechanisms that achieve chirality are still widely unknown.

Previous studies have shown that *Drosophila* myosin-I isoforms myosin-1C (myo1C) and myosin-1D (myo1D) are involved in establishing chirality of certain organs (Petzoldt). In addition, the overexpression of either isoform into a non-chiral tissue induces chirality, with the expression two myosin-I isoforms resulting in organs with opposite handedness (Lebreton). To add on, a possible interaction between myo1D and cell-cell adhesion proteins such as DE-cadherin and/or beta-catenin have been suggested, where myo1C is thought to inhibit this interaction. In this project, we study the possible role of *Drosophila* myo1D at the molecular level that could translate to organ chirality.

The potential of myo1D binding to DE-cadherin could not only imply that the motor directly applies forces between cells, but also induces directional cues that induce chirality. Ongoing biochemical studies of these myosin-Is suggest that myo1D is a high-duty ratio motor, meaning that it dwells in strong-binding states for most of its ATPase cycle. This kinetic feature points to the possibility that myo1D binds to cell-cell adhesion sites and creates a twisting torque that could translate to neighboring cells to promote tissue/organ chirality. Our goal is to directly test the possibility that myo1D can bind DE-cadherin and power the motility of actin filaments.

Materials and Methods: Using an *in vitro* motility technique we call actin gliding assays, we reconstituted actin movement on supported lipid bilayers. Experiments were performed with bilayers containing PtdIns(4,4)P_2 (PIP2) and/or the cytoplasmic domain of hist-tagged DE-cadherins bound DGS-NTA (Ni) lipids which bind to our His-tagged cytoplasmic DE-cadherin construct. We added myo1D and a final solution containing fluorescently labeled actin filaments to detect and control for myosin-cadherin attachment by observing the attachment and movement of the actin filaments.

Results and Discussion: To build this intricate *in vitro* system, a control condition previously done in the lab was performed, composed of a lipid bilayer of PIP2 which binds to the tail domain of the myosin-Is. We reproduced binding and motility of actin filaments in these conditions. Preliminary experiments with DGS-NTA (Ni) with and without PIP2 lipids show limited actin filament binding, but further experimentation is needed to confirm this finding as mixed results were obtained. Though several attempts at introducing out Hist-tagged DE-cadherin into the DGS-NTA (Ni) system have been made, no reliable results have yet been established.

Conclusions: More troubleshooting and experimentation is needed to make accurate conclusions about our experiments.

References

Petzoldt, A. G., Coutelis, J.-B., Géminard, C., Spéder, P., Suzanne, M., Cerezo, D., & Noselli, S. (2012). DE-Cadherin regulates unconventional Myosin ID and Myosin IC in Drosophila left-right asymmetry establishment. In Development (Vol. 139, Issue 10, pp. 1874–1884). The Company of Biologists. https://doi.org/10.1242/dev.047589

Lebreton, G., Géminard, C., Lapraz, F., Pyrpassopoulos, S., Cerezo, D., Spéder, P., Ostap, E. M., & Noselli, S. (2018). Molecular to organismal chirality is induced by the conserved myosin 1D. In Science (Vol. 362, Issue 6417, pp. 949–952). American Association for the Advancement of Science (AAAS). https://doi.org/10.1126/science.aat8642